Proceedings of the 2018 IEEE
International Conference on Robotics and Biomimetics
December 12-15, 2018, Kuala Lumpur, Malaysia

Robot-Assisted Rehabilitation System Based on SSVEP Brain-Computer Interface for Upper Extremity

Yaqi Chu, Xingang Zhao, *Member, IEEE*, Yijun Zou, Weiliang Xu, and Yiwen Zhao

***Abstract*—Traditional rehabilitation therapies have limited effect on the motor recovery for a tetraplegia patient. Brain-computer interface (BCI) systems allow patients to send commands or intents to control external devices without depending on the normal way of peripheral nerves and muscles. And hence it can provide an alternative control and communication method with a potential to replace, restore, even reinforce lost movement ability for individuals with neurological damages. In the study, we proposed a robot-assisted rehabilitation system for upper extremity based on non-invasive electroencephalogram (EEG) BCI, which enables the injured upper extremity to achieve motor function. Six participants conducted three speed modes of movement with a BCI-controlled robot. The steady-state visual evoked potentials (SSVEPs) was adopted to establish the BCI system. Experimental results of the healthy participants were analyzed to indicate the feasibility of a BCI-driven robot-assisted rehabilitation system, with an average accuracy of about 80 %. This study gives a preliminary evidence that the integrated robot-assisted rehabilitation system combined with SSVEP-based BCI will make future rehabilitation therapy more effective.**

I. Introduction

THE Cerebral Palsy (CP), Amyotrophic Lateral Sclerosis (ALS), Spinal Cord Injury (SCI), and brain stroke can result in the loss of the movement function for individuals with partial or severe paralysis, which seriously affected quantity of daily life in their homes, workplaces, and communities. However, with effective rehabilitation therapies, impaired subjects can partially restore movement ability and perform their daily life. Currently, biomedical treatments and physical therapies were the most widely used approaches [1], which involve rehabilitation physicians to help the patients to exercise the affected limbs or body sides. Unfortunately, traditional physical method is high labor cost and needs one-to-one manual exercise with physicians [2]. Furthermore, the evaluation of rehabilitation performance is usually difficult. Hence, these treatments provide a limited degree of motor function rehabilitation. Compared with the physical therapy, the robot-assisted method can realize high-intensity, repetitive and task-oriented exercise for injured limbs, and also provides novel exercises that are not available in other therapies [3]. Researches have shown that the robotic rehabilitation therapy can restore and improve the function of hemiparetic upper extremity after neurological injuries, such as chronic stroke [4].

Many groups and research institutes have developed robotic rehabilitation prototypes, including MIT-MANUS [5], Bi-Manu-Track [6], ARM Guide [7], and MIME [8]. Although these researches have presented some efficacy and advantages of the robot-assisted methods for movement recovery in the lower or upper limbs, no direct interaction was existed between the patients' volitional movement and the robot system. The patients just only follow the preset procedure passively in exercise period, which could not entirely excite their initiatives and enthusiasm of the movement.

During the area of brain signal process, recent researches have enabled people with destructive motion disabilities to directly utilize EEG signal to control or communicate with external environments. This brain-computer/machine interface (BCI/BMI) system can interpret EEG signal as instructions to control external devices directly (e.g., robot-assisted device) [9] and then bypass the normal motor control pathways. At present, many BCI/BMI applications have been established in various fields, such as object operation in 2D [10] or 3D space [11], remote device teleoperation [12], biometric identification [13] and emotion recognition [14]. More prominently, the BCI/BMI technology has been already adopted to drive prosthetic devices for limbs rehabilitation [15], [16]. These non-invasive BCI/BMI systems can facilitate the impaired muscle control of patients by using their current intentions. Moreover, the BCI-driven neurological prostheses provide a feasible rehabilitation scheme for movement function recovery. In brief, the robot-assisted rehabilitation systems combined with a BCI

This work was supported by the Nation Natural Science Foundation of China (Grants nos. 61503374 and 61573340), and in part by the Frontier Science research project of the Chinese Academy of Sciences (Grant No. QYZDY-SSW-JSC005).

Yaqi Chu and Yijun Zou are with the State Key Laboratory of Robotics, Shenyang Institute of Automation (SIA), Chinese Academy of Sciences (CAS); Institutes for Robotics and Intelligent Manufacturing, Chinese Academy of Sciences (CAS), Shenyang, Liaoning, 110016 China, and also with University of Chinese Academy of Sciences (UCAS), Beijing, China (e-mail: {chuyaqi, zouyijun}@sia.cn).

Xingang Zhao and Yiwen Zhao are with the State Key Laboratory of Robotics, Shenyang Institute of Automation (SIA), Chinese Academy of Sciences (CAS), and also with Institutes for Robotics and Intelligent Manufacturing, Chinese Academy of Sciences (CAS), Shenyang, Liaoning, 110016 China (zhaoyw@sia.cn; corresponding author to provide e-mail: zhaoxingang@sia.cn).

Weiliang Xu is with the State Key Laboratory of Robotics, Shenyang Institute of Automation (SIA), Chinese Academy of Sciences (CAS) and also with the Department of Mechanical Engineering, University of Auckland, Auckland, 1142 New Zealand (e-mail: p.xu@auckland.ac.nz).

978-1-7281-0377-8/18/$31.00 © 2018 IEEE

are expected to produce well effect on movement recovery, especially for severely-impaired subjects.

The motor imagery-based BCI (MI-BCI) has been applied in robotic rehabilitation for upper extremity [9]. The neurophysiological background behind MI-BCI is that somatosensory stimulation [18] or motor imagery [17] oscillates the relevant sensorimotor rhythm in spatial localization [19]. However, some fatal limitations are existed in this MI-based BCI system, such as apparently lower prediction accuracy, fewer predictable movements and longer calibration time. Besides, the huge inter-subject variability of the MI EEG signal is also one of the challenges [20].

Considered the deficiencies of motor imagery signals, we chose Steady-state Visual Evoked Potentials (SSVEPs) response as the input signals of BCI. The SSVEP-EEG signal is a response to an external stimulus flashing at a frequency from the visual cortex [21]. Compared with other types of BCI, an SSVEP-BCI system has the merits of higher accuracy and information transfer rate (ITR), less individual discrepancy, and no or shorter calibration time [22]. Furthermore, the SSVEP EEG is more suitable for a BCI-driven robotic rehabilitation system due to their reliability and robustness.

In this paper, an integrated robot-assisted system combined with SSVEP-BCI was presented for upper extremity rehabilitation. The BCI-driven robotic rehabilitation system interpreted the mental intentions as commands to control the rehabilitation robot to exercise the impaired upper extremity in a similar way with the physical therapy. The overall article structures are presented as follows. The section II introduces the framework of BCI-driven robotic rehabilitation system. Then, a detailed SSVEP-based BCI system is given in section III. The experimental study of BCI-driven robotic rehabilitation is presented in section IV. And then, some results are shown in section V. Finally, section VI gives the conclusions and future work.

II. Overall Framework Of The System

A robotic rehabilitation system combined with a non-invasive SSVEP-BCI was constructed for the upper extremity in this study. The schematic diagram of the overall framework is illustrated in Fig. 1. When the patient stares at a specific flickering stimulation, the induced SSVEP signals are collected from the relevant area at the visual cortex of the scalp. After preprocessing, feature extraction and pattern classification, the individuals' intention about which stimulation is being focused on can be detected. Then a command is generated by coding the detected intention, which triggers rehabilitation robot to assist upper extremity to execute movement task according to her or his own willingness. This research needs an offline BCI calibration phase, where subject-specific BCI system is trained with raw SSVEP EEG signals. Finally, the online rehabilitation phase for this integrated system with SSVEP-BCI is executed and evaluated in the real-time way.

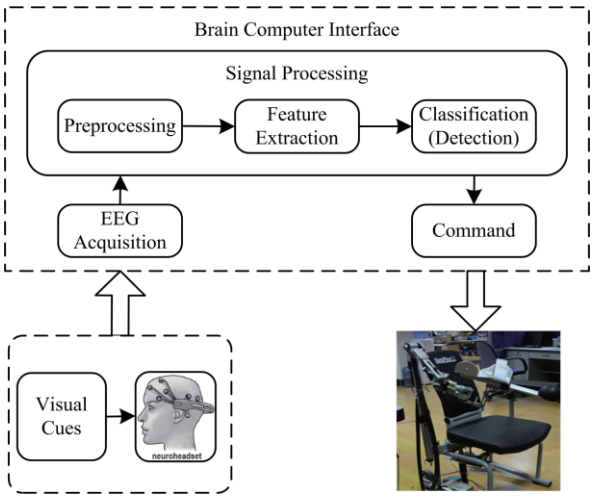

Fig. 1. The framework of the integrated upper extremity robotic rehabilitation system combined with SSVEP-based Brain-Computer Interface (SSVEP-BCI).

In this study, the experimental procedures were approved by the local ethics committee, and all participants signed their informed consent forms before the experiment. Six participants with the age 25.0 ± 1.7 years (mean ± standard deviation, two females, four males) were recruited in the BCI-driven robot experiment. Since this preliminary study gives a validation experiment, all the participants are able-bodied without a history of neurological injury. Moreover, the participants have no previous experience in the SSVEP-BCI experiment.

III. SSVEP Based BCI System

A. Visual Cues Design

How to design the visual cues is the extremely important problem for the SSVEP-BCI system, due to the fact that the amplitude and the phase of the SSVEP signal depends on the shape, flashing frequency, and intensity of the repetitive visual cues [23].

In some literatures, the visual cues can be designed and presented by various shapes in a cathode ray tube (CRT) or liquid crystal display (LCD) monitor. Limited by the refresh rate of the computer monitor, the flickering frequency of the visual cues cannot be designed casually. Moreover, the stimulus with flickering frequency between 5 and 27 Hz can induce stronger SSVEP signals from the visual cortex typically, with the strongest SSVEP induced at the frequency of 15 Hz [24]. Generally, for the computer monitors with 60 Hz refresh rate, the frequencies of 7.5 Hz, 10 Hz, 12 Hz, 15 Hz and 20 Hz can be utilized to design the visual stimulus. However, the SSVEP response induced by the fundamental flickering frequency can be corrupted by the harmonic frequency. Consequentially, the BCI algorithm cannot correctly classify which SSVEP signal belongs to the fundamental frequency or the harmonic frequency. To sum up, in this study, three frequencies with 20 Hz, 15 Hz and 12 Hz were selected to induce strong and high separable SSVEP signal. Three square stimulators with triangular distribution were designed, which oscillated between red and black color (Fig. 2). The flashing frequency of the square is encoded by the programmed codes.

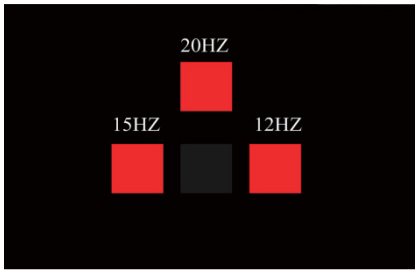

Fig. 2. The design of three visual stimulus. The cues were presented by the square shape, which flashes between red and black at a frequency. The left square flashes by 15 Hz frequency, the top square flashed by 20 Hz frequency and the right square flashes by 12 Hz frequency. The black square in the center represents no flickering frequency.

B. BCI Procedures

1) SSVEP Signal Collection: The Emotiv EPOC headset was used in this study, which is a high-fidelity EEG device. It has 14 EEG signal collecting channels (AF3, F7, F3, FC6, F4, F8, AF4, FC5, T7, P8, T8, O1, O2, respectively), and 2 reference electrodes (CMS/DRL). The layouts of electrodes are placed on the scalp roughly according to the international 10-20 positioning system. The headset digitally sampled at 128 HZ with a resolution of 14 bits.

2) SSVEP Signal Filtering: Usually, raw acquired SSVEP signals are contained by various artifacts, such as sEMG signal from face, eye noise and motion artifacts, which should be eliminated by filtering procedure. To remove the DC component and low frequency drift of the signal, a Butterworth filter with fifth-order and cut-off frequency 2 Hz was adopted to filter the raw SSVEP. Then, a notch filter was designed to filter the 50 Hz power line interference. Furtherly, the spatial filtering algorithm (common spatial patterns, CSP) was applied to improve the signal-noise-ratio of the SSVEP with the interesting frequency bands.

The detailed CSP algorithm can be described as the following. The single-trial SSVEP signal is presented by a matrix A with the dimensionality $N \times M$, where N is the channel and M is the sampled data. For the A, the covariance matrix can be obtained by

$$C = \frac{AA^T}{tr(AA^T)}, \tag{1}$$

where $tr(\bullet)$ denotes the matrix trace and T is the transpose operator. For two class of the SSVEP, the covariance matrix can be computed as C_1 and C_2 respectively. Then, the entire spatial covariance matrix R_{sum} can be summed and factorized in a way of eigenvalue decomposition.

$$R_{sum} = C_1 + C_2 = U\lambda U^T, \tag{2}$$

where λ is eigenvalues which are sorted in descending order. A whitening matrix P is constructed as

$$P = \sqrt{\lambda^{-1}} U^T. \tag{3}$$

Then covariance matrix C_1 and C_2 are transformed by the P

$$S_1 = PC_1P^T,\ S_2 = PC_2P^T. \tag{4}$$

We can find that the transformed matrix S_1 and S_2 have dual eigenvectors.

$$S_1 = B\lambda_1 B^T \tag{5}$$

$$S_2 = B\lambda_2 B^T \tag{6}$$

$$\lambda_1 + \lambda_2 = I \tag{7}$$

where I is the identity matrix. For the dual problem, the eigenvector corresponding to the largest eigenvalue from S_1 has smallest eigenvalue for S_2. Finally, the optimal spatial filtering matrix can be formulated by using the first k columns and the last k columns of B as B_1

$$W = B_1{}^T P. \tag{8}$$

In our experiment, the selected columns were setting 2. Hence, the CSP filter converts the 14 channels into 2 channels.

3) Power Feature Extraction: The feature of the power spectrum was extracted from the SSVEP signals with interested frequency band, which including 11.75-12.25 Hz for 12 Hz flickering frequency, 14.75-15.25 Hz for 15 Hz flickering frequency, 19.75-20.25 Hz for 20 Hz flickering frequency, respectively. For a trial with 7 s length, the Fast Fourier Transform (FFT) was applied to 0.5 s intervals of the EEG signals every 0.1 s and the power for each frequency was then computed using squared values.

4) LDA Classifier Design: In the view of three EEG classes in this study, three LDA classifiers based on pairwise strategy were used. For each LDA classifier, the output was a logistic value, representing that the likelihood of which the flashing cues the SSVEP belongs. A voting strategy was conducted among these three LDA classifiers to increase the prediction accuracy. A final class was determined by the majority output of the three LDA. Once the class of the SSVEP signal has been identified, it can be associated with a command which is sent to a computer in order to control peripheral devices.

C. Indicator of SSVEP-BCI Algorithm

Generally, the recognition accuracy is an important indicator for evaluating the BCI algorithm. However, for the SSVEP-based BCI system, the indicator of information transfer rate (ITR) is also used to assess the performance. The ITR index can be computed by

$$ITR = \log_2 c + a\log_2 a + (1-a)\log_2(\frac{1-a}{c-1}), \tag{9}$$

where a is the recognition accuracy and c is the number of class (i.e., the number is 3 in our experiment). The unit of the ITR index is bits per minute (bpm).

IV. Experimental Procedure

A. Experimental Setup

Fig. 3 presents the experimental scene of the proposed rehabilitation system. The overall system includes EEG signal acquisition section, computer interface, and rehabilitation robot (exoskeletal mechanical arm, motor drive, and motor actuator). The EPOC headset captured the EEG signals and the computer

interface processed the obtained signals and got an advanced command by the designed SSVEP-BCI algorithm. The command was mapped to specific motor rehabilitation mode. In the paper, a 3-DOF upper extremity rehabilitation robot was applied, which could complete extending/flexing movement of should joint, outreach/adduction of should joint, and extending/flexing movement of elbow joint.

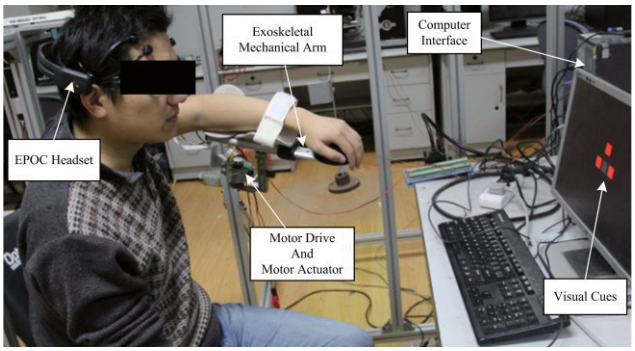

Fig. 3. The setup of the proposed SSVEP-BCI robotic rehabilitation system for upper extremity.

B. Experimental Protocol

The robotic rehabilitation system has three periodic modes of operation for the elbow joint of the upper extremity: a) fast speed motor mode; b) medium speed motor mode; c) slow speed motor mode. The trajectory positions of these modes were already pre-determined. Three stimulation squares with different flickering frequencies were corresponding respectively to various speed modes, such as 12 Hz square corresponds to slow mode, 15 Hz square represents medium mode and 20 Hz square represents fast mode, respectively. The total experimental procedure included two phases for each participant: the calibration phase and online rehabilitation phase. Firstly, the calibration phase was conducted to offline train and learn a decoder for the SSVEP-BCI. Then, the online phase carried out the BCI-driven robotic rehabilitation experiment in real time. The calibration phase acquires a total of 32 trials of SSVEP signals that comprised 24 trials of flashing square with different frequencies and 8 trials with no flickering square randomly. Firstly, a 1 s visual cue with no flickering on the screen was presented for the participants which sat in a comfortable seat. With that, the participants were recommended to focus their eyes on the cued square with a yellow arrow indicated. The flickering square lasted 7 s, followed by random interval time between 4 s and 6 s. Then, the participants can shift their attention to the next indicated square. The duration of each SSVEP trial was approximately 15 s. 1 minute of rest was given in between every 8 trials.

In the calibration phase, we constructed a subject-specific SSVEP-BCI decoder for using in the subsequent rehabilitation phase. In the rehabilitation phase, the participant's upper extremity was closely strapped to the exoskeletal mechanical arm of the robot. The participant was firstly given with a 1 s visual cue, then a yellow arrow would indicate the participant to gaze the oscillating stimulus with specific frequency. If the rehabilitation purpose was recognized during the 5 s focusing period, the 3-DOF robot immediately assist the participant in periodically moving the upper extremity to track a pre-determined trajectory. According to the detected rehabilitation intent, the relevant speed motor mode was selected. The motor drive decoded motor commands by using position-based trajectory learning framework. At the same time, the potentiometer and encoder in the motor will transport the acquired angle and location data to the PC through standard RS232 serial port, to real-time adjust the motor commands.

V. Experiment Results and Analysis

A. Offline BCI Calibration Results

The offline BCI calibration phase established a subject-specific BCI model for each subject. To prevent the over-fitting of the LDA classifier and ensure that the obtained offline recognition accuracy generalizes to online phase, a 10-fold cross-validation approach was utilized to compute and train optimal LDA classifier with better parameters. In this study, a strategy of one-versus-the-rest was applied in the design of the pairwise LDA classifier. For each subject, three LDA classifiers (LDA-1, LDA-2, and LDA-3) were modeled for mainly recognizing each SSVEP signal with 12 Hz, 15 Hz and 20 Hz, respectively. The results of recognition accuracy and the relative ITR index for the six participants were showed in the Table I. From the Table I, we can see that the classification accuracies for each LDA classifier and subject vary from 77.20 % to 92.40 %. The mean accuracies for LDA-1, LDA-2, and LDA-3 were 80.08±1.52 %, 82.30±1.60 % and 85.80±1.67 % respectively, with an average BCI accuracy of about 80 %. Moreover, the average ITR index for all the six subjects was 28.60±5.45 bits/min.

Particularly, we can see that the mean accuracy of the LDA-3 classifier was slightly better than the other two classifiers (LDA-1 and LDA-2). It could be the reason that the stable and preferable SSVEP signals can be induced by flickering square with 20 Hz. And then, the extracted power features during the relevant frequency band was more separable. Additionally, the performance of the LDA-1 for identifying 12 Hz flickering square was worse for subject 3 and 5, with accuracy of 78.10±1.50 % and 78.15±1.50 %, respectively. This may be caused by the interference of the alpha frequency band (8-13 Hz). The interesting frequency band (11.75-12.25 Hz) for 12 HZ SSVEP signals was corrupted by alpha frequency band, which the EOG signal may be resident in the SSVEP signals. However, the decoding algorithm for the SSVEP signal was available and promising to construct an effective BCI system.

TABLE I
The Classification Results of The Six Subjects in Calibration phase

Subject	LDA-1 (%)	LDA-2 (%)	LDA-3 (%)	Average ITR (bmp)
S1	80.40±1.38	82.50±1.42	78.24±1.35	26.20±5.80
S2	83.25±1.42	79.85±1.42	85.45±2.64	28.90±5.15
S3	78.10±1.50	77.20±1.40	92.00±1.52	25.45±5.58
S4	80.00±2.00	78.55±2.25	78.20±1.45	27.20±6.00
S5	78.15±1.50	88.00±1.50	92.40±1.41	28.05±6.00
S6	80.55±1.30	87.65±1.62	88.50±1.60	28.60±5.45
Mean	80.08±1.52	82.30±1.60	85.80±1.67	27.40±5.67

B. *Online Experimental Results*

In online rehabilitation phase, subjects can focus attention on the three visual stimuli by their initiatives. Thereby, three speed modes of motions can be executed by the upper extremity robot. During each mode, the subject was assisted by the robot to perform 5 s periodic extending and flexing movement of the elbow joint. The tracking trajectory of the robot can be obtained by sensors. From the Fig. 4 to Fig. 6, the trajectory tracking performance of the subject 1 was presented for slow mode, medium mode and fast mode, respectively. The red line denotes the actual trajectory of elbow joint assisted by the robot. The black line denotes the desired trajectory of elbow joint. We can see that the robot can track a desired trajectory by using SSVEP-based BCI.

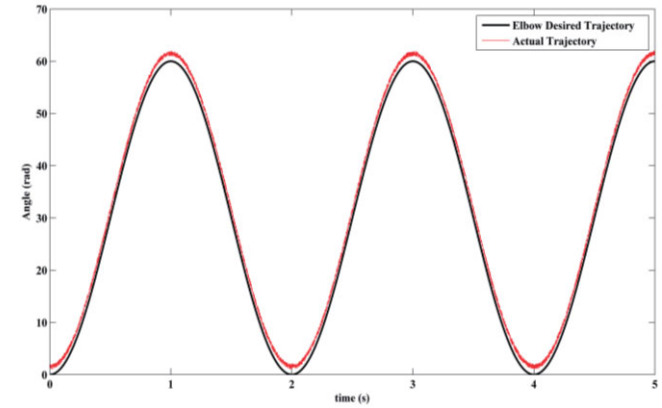

Fig. 4. The trajectory tracking result of slow motor mode (0.5 HZ).

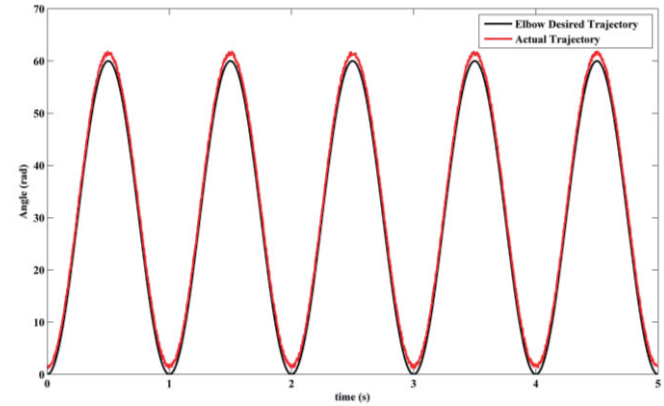

Fig. 5. The trajectory tracking result of medium motor mode (1.0 HZ).

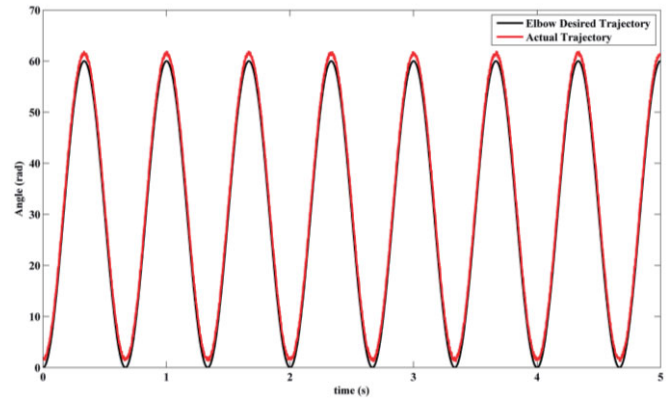

Fig. 6. The trajectory tracking result of fast motor mode (1.5 HZ).

The angle tracking errors of three motor modes were given in the Fig. 7, Fig. 8 and Fig. 9, respectively. The error was the difference value between the desired angle trajectory and the actual motion of the upper limb. The average tracking error was 1.5047 rad for slow mode, 1.5127 rad for medium mode, 1.5130 rad for fast mode. These indicate that the rehabilitation robot can assist the upper extremity to track a desired trajectory with a small error.

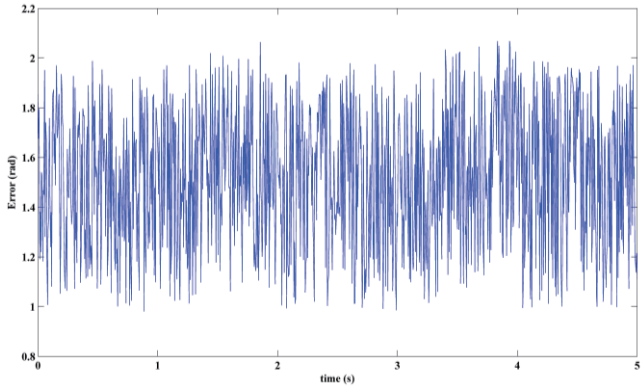

Fig. 7. The tracking error of slow motor mode (0.5 HZ) by the robot.

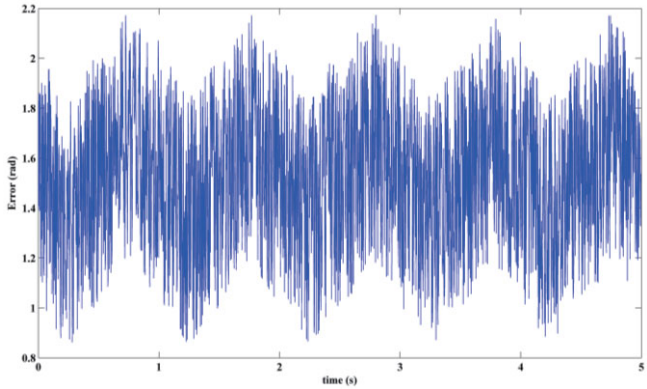

Fig. 8. The tracking error of medium motor mode (1.0 HZ) by the robot.

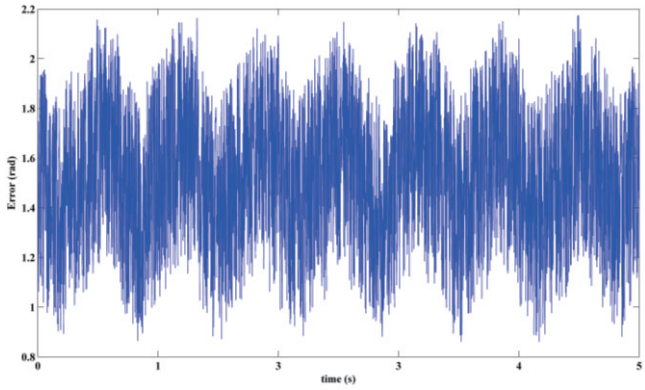

Fig. 9. The tracking error of fast motor mode (1.5 HZ) by the robot.

Equally, the performance of the online BCI-driven robotic rehabilitation system and motor mode execution rate was obtained for six subjects. For motor mode implementation rate, it is a proportion of successful completing motor mode (see in Table II). The performance of online robotic rehabilitation experiments based on SSVEP-BCI shows that the proposed system is available to assist the subject's upper extremity to follow a desired trajectory. During all the participants, the

TABLE II
PERFORMANCE OF THE ONLINE BCI-DRIVEN ROBOTIC SYSTEM

Subject	Slow Mode (%)	Medium Mode (%)	Fast Mode (%)
S1	72.20	68.20	70.50
S2	70.50	74.00	80.48
S3	80.44	83.26	87.50
S4	58.10	60.15	60.50
S5	82.12	82.10	82.00
S6	78.08	82.50	79.00
Mean	73.57±8.85	75.04±9.41	76.66±9.65

completion rates for each speed motor mode vary from 58.10 % to 87.50 %. The mean performance for slow mode, medium mode and fast mode was 73.57±8.85 %, 75.04±9.41 % and 76.66±9.65 %, respectively. Compared with offline results, the online experimental results were decreased due to the fact that different factors interfered the performance of the online SSVEP-BCI, such as data missing caused by loose channel and external electromagnetic artifacts. In addition, compared with other five subjects, the performance for the subject 4 was worse, such as the 58.25 % accuracy was only obtained for the slow mode. The possible reason is that the induced SSVEP signals are not stable and feasible when he didn't focus his attention.

VI. CONCLUSION AND PROSPECT

In this paper, an integrated rehabilitation robot system combined with SSVEP-based BCI system was proposed. And the subject's movement intention was interpreted as commands to drive the robot system to assist the upper extremity to exercise like a physical therapy. Due to it is a preliminary research, the proposed BCI-driven robotic rehabilitation system was conducted during six unimpaired participants. The performance of the SSVEP-based BCI is stable, achieving mean accuracy of over 80 % in the group level of six subjects. However, the recognition rate of SSVEP-BCI should be further improved. In the future work, a study that sought to assess whether attention to real-world activity impaired performance in a BCI based on SSVEP response elicited by visual attention. Moreover, the asynchronous BCI system should be furtherly developed instead of this synchronization SSVEP-based BCI. An important future direction is validating this integrated rehabilitation system with a group of patients with upper limb paralysis.

ACKNOWLEDGMENT

The authors acknowledge Yingli Li *et al.* for participating this experiments.

REFERENCES

[1] P. Langhorne, F. Coupar, and A. Pollock, "Motor recovery after stroke: a systematic review," *The Lancet Neurology*, vol. 8, no. 8, pp. 741-754, 2009.

[2] S. Federici, F. Meloni, M. Bracalenti, and M. L. De Filippis, "The effectiveness of powered, active lower limb exoskeletons in neurorehabilitation: a systematic review," *NeuroRehabilitation*, vol. 37, no. 3, pp. 321-340, 2015.

[3] A. Basteris, S. M. Nijenhuis, A. H. Stienen, J. H. Buurke, G. B. Prange, and F. Amirabdollahian, "Training modalities in robot-mediated upper limb rehabilitation in stroke: a framework for classification based on a systematic review," *J. Neuroeng. Rehabil.*, vol. 11, no. 1, pp. 111, 2014.

[4] J. M. Veerbeek, A. C. Langbroek-Amersfoort, E. E. Van Wegen, C. G. Meskers, and G. Kwakkel, "Effects of robot-assisted therapy for the upper limb after stroke: a systematic review and meta-analysis," *Neurorehab. Neural Re.*, vol. 31, no. 2, pp. 107-121, 2017.

[5] H. I. Krebs, N. Hogan, B. T. Volpe, M. L. Aisen, L. Edelstein, and C. Diels, "Overview of clinical trials with MIT-MANUS: a robot-aided neuro-rehabilitation facility," *Technol. Health Care*, vol. 7, no. 6, pp. 419-423, 1999.

[6] S. Hesse, G. Schulte-Tigges, M. Konrad, A. Bardeleben, and C. Werner, "Robot-assisted arm trainer for the passive and active practice of bilateral forearm and wrist movements in hemiparetic subjects," *Arch. Phys. Med. Rehabil.*, vol. 84, no. 6, pp. 915-920, 2003.

[7] D. J. Reinkensmeyer, L. E. Kahn, M. Averbuch, A. McKenna-Cole, B. D. Schmit, and W. Z. Rymer, "Understanding and treating arm movement impairment after chronic brain injury: progress with the ARM guide," *J. Rehabil. Res. Dev.*, vol. 37, no. 6, pp. 653-662, 2000.

[8] C. G. Burgar, P. S. Lum, P. C. Shor, and H. F. Machiel Van der Loos, "Development of robots for rehabilitation therapy: the Palo Alto VA/Stanford experience," *J. Rehabil. Res. Dev.*, vol. 37, no. 6, pp. 663-673, 2000.

[9] J. Meng, S. Zhang, A. Bekyo, J. Olsoe, B. Baxter, and B. He, "Noninvasive electroencephalogram based control of a robotic arm for reach and grasp tasks," *Sci. Rep.*, 6: 38565, 2016.

[10] T. Ma, H. Li, L. Deng, H. Yang, X. Lv, P. Li, *et al.*, "The hybrid BCI system for movement control by combining motor imagery and moving onset visual evoked potential," *J. Neural Eng.*, 14: 026015, 2017.

[11] K. LaFleur, K. Cassady, A. Doud, K. Shades, E. Rogin, and B. He, "Quadcopter control in three-dimensional space using a noninvasive motor imagery-based brain–computer interface," *J. Neural Eng.*, vol. 10, 2013.

[12] J. Lin, and Z. Jiang, "Implementing remote presence using quadcopter control by a non-invasive BCI device," *Comput. Sci. Inform. Technol.,* vol. 3, pp. 122-126, 2015.

[13] R. Palaniappan, "Two-stage biometric authentication method using thought activity brain waves," *Int. J. Neural Syst.*, vol. 18, pp. 59-66, 2008.

[14] J. I. Padilla-Buritica, J. D. Martinez-Vargas, and G. Castellanos-Dominguez, "Emotion Discrimination Using Spatially Compact Regions of Interest Extracted from Imaging EEG Activity," *Front. Comput. Neurosci.*, vol. 10, 2016.

[15] L. R. Hochberg, D. Bacher, B. Jarosiewicz, N. Y. Masse, J. D. Simeral, J. Vogel, *et al.*, "Reach and grasp by people with tetraplegia using a neurally controlled robotic arm," *Nature*, vol. 485, pp. 372-375, 2012.

[16] T. Ma, H. Li, L. Deng, H. Yang, X. Lv, P. Li, *et al.*, "The hybrid BCI system for movement control by combining motor imagery and moving onset visual evoked potential," *J. Neural Eng.*, vol. 14, 2017.

[17] M. Stavrinou, L. Moraru, L. Cimponeriu, S. Della Penna, and A. Bezerianos, "Evaluation of cortical connectivity during real and imagined rhythmic finger tapping," *Brain Topogr.,* vol. 19, no. 3, pp. 137-145, 2007.

[18] H. Yuan and B. He, "Brain-computer interfaces using sensorimotor rhythms: current state and future perspectives," *IEEE Trans. Biomed.* Eng., vol. 61, pp. 1425-1435, 2014.

[19] B. He, B. Baxter, B. J. Edelman, C. C. Cline, and W. W. Ye, "Noninvasive brain-computer interfaces based on sensorimotor rhythms," *Proceedings of the IEEE*, vol. 103, pp. 907-925, 2015.

[20] B. Blankertz, S. Lemm, M. Treder, S. Haufe, and K. R. Müller, "Single-trial analysis and classification of ERP components-a tutorial," *Neuroimage*, vol. 56, pp. 814-825, 2011.

[21] M. Nakanishi, Y. Wang, X. Chen, Y. T. Wang, X. Gao, and T. P. Jung, "Enhancing detection of SSVEPs for a high-speed brain speller using task-related component analysis," *IEEE Trans. Biomed. Eng.*, vol. 65, pp. 104-112, 2018.

[22] X. Zhao, Y. Chu, J. Han, and Z. Zhang, "SSVEP-based brain-computer interface controlled functional electrical stimulation system for upper extremity rehabilitation," *IEEE Trans. Syst. Man, Cybern. Syst.*, vol. 46, pp. 947-956, 2016.

[23] Z. Wu, Y. Lai, Y. Xia, D. Wu, and D. Yao, "Stimulator selection in SSVEP based BCI," *Med. Eng. Phys.*, vol. 30, no. 8, pp. 1079–1088, Oct. 2008.

[24] X. Chen, Y. Wang, M. Nakanishi, X. Gao, T. P. Jung, and S. Gao, "A high-speed spelling with a noninvasive brain-computer interface," *Proc. Natl. Acad. Sci. USA*, vol. 112, pp. 6058-6067, 2015.